

# Survival probability in a quenched Majorana chain with an impurity

Atanu Rajak

*CMP Division, Saha Institute of Nuclear Physics,  
1/AF Bidhannagar, Kolkata 700 064, India and*

*Department of Physics, Jack and Pearl Resnick Institute, Bar-Ilan University, Ramat-Gan 52900, Israel*

Tanay Nag

*Department of Physics, Indian Institute of Technology Kanpur, Kanpur 208 016, India*

We investigate the dynamics of a one-dimensional  $p$ -wave superconductor with next-nearest-neighbor hopping and superconducting interaction derived from a three-spin interacting Ising model in transverse field by mapping to Majorana fermions. The next-nearest-neighbor hopping term leads a new topological phase containing two zero-energy Majorana modes at each end of an open chain, compared to a nearest-neighbor  $p$ -wave superconducting chain. We study the Majorana survival probability (MSP) of a particular Majorana edge state when the initial Hamiltonian ( $H_i$ ) is changed to the quantum critical as well as off-critical final Hamiltonian ( $H_f$ ) which additionally contains an impurity term ( $H_{imp}$ ) that breaks the time-reversal invariance. For the off-critical quenching inside the new topological phase with  $H_f = H_i + H_{imp}$ , and small impurity strength ( $\lambda_d$ ), we observe a perfect oscillation of the MSP as a function of time with a single frequency (determined by the impurity strength  $\lambda_d$ ) that can be analyzed from an equivalent two-level problem. On the other hand, the MSP shows a beating like structure with time for quenching to the phase boundary separating the topological phase (with two edge Majoranas at each edge) and the non-topological phase where the additional frequency is given by inverse of the system size. We attribute this behavior of the MSP to the modification of the energy levels of the final Hamiltonian due to the application of the impurity term.

PACS numbers: 74.40.Kb, 74.40.Gh, 75.10.Pq

## I. INTRODUCTION

In the rapidly growing field of research in topological quantum computation, quantum information processing and decoherence, Majorana fermions, introduced by Ettore Majorana [1] in the context of the existence of real solution of Dirac equation, play a key role [2–5]. The theoretical prediction of the existence of zero-energy Majorana edge modes in an open chain has paved the way for understanding of various topological character for a system like one-dimensional spinless  $p$ -wave superconductor [6–14]. An interesting proposal has been made for achieving the Majorana states by the proximity effect between the surface state of a strong topological insulator and a  $s$ -wave superconductor [15]. A topological phase is characterized by a topological invariant number, for example, the number of zero-energy Majorana edge modes in the case of  $p$ -wave superconducting chain. This number does not change unless the system goes from one topological phase to the other separated by a quantum critical line, as also happens in a topological insulators [16, 17]. The zero-energy Majorana modes have recently been found experimentally in nanowires coupled to superconductors [18–22]; although there exists some theoretical contradictions with the experimental observation [23]. An experimental realization of the hybridization of Majorana fermions has also been observed through the zero-bias anomalies in the differential conductance of an InAs nanowire coupled to superconductor [24].

On the other hand, given the recent interest in the

non-equilibrium quenching dynamics of quantum many body systems across QCPs, the investigations of different topological systems in out-of-equilibrium have become a prime research field [25–38]. In this connection, the dynamics of an edge state has been extensively investigated in one [39] and two dimensional [40] topological systems. Recently, the dynamics of the Majorana edge state also has been studied following a sequence of quenches in an one-dimensional system [41]. It is noteworthy to mention that the dynamical generation [12], formation and manipulation [42] of Majorana edge states for a driven system have also studied extensively. Additionally, the theoretical prediction of an adiabatic transport of an edge Majorana through an extended gapless region has been made in a  $p$ -wave superconducting chain with complex hopping term [43].

We consider here a generalized one-dimensional Ising model in a transverse field with a three-spin interaction term [44] which can be written in term of fermionic operators using the Jordan-Wigner transformation. This longer-range interacting model has a richer phase diagram containing an extra topological phase with two zero-energy Majorana edge modes [45] as compared to the one-dimensional  $p$ -wave superconductor which is fermionized version of the transverse field XY model [12]. If we break the time-reversal symmetry of the above Hamiltonian by adding an impurity term, the Majorana modes at one end of the chain vanishes in the topological phase with two Majorana modes depending on the nature of the impurity term [45]. Our main aim here is to

investigate the fate of a Majorana edge state under time evolution governed by the Hamiltonian with an impurity that destroys the edge state in equilibrium.

In particular, we investigate the Majorana survival probability (MSP) as a function of time following both critical and off-critical quenches in the presence of an impurity term in the final Hamiltonian. We show that this impurity term modifies the energy levels of the final Hamiltonian and consequently an extra time scale appears in the system which is reflected in the behavior of the MSP. Most Interestingly, for weak impurity strength, we find that MSP exhibits perfect temporal oscillation with a single frequency following an off-critical quench inside the topological phase carrying two edge Majoranas; the oscillation frequency is determined by the inverse of impurity strength. In this connection, we note that recently the single frequency oscillation in entanglement spectrum also has been found for a two-impurity Kondo model by suddenly changing the RKKY interaction strength [46]. On the other hand, MSP shows a beating like structure when the system is quenched up to a QCP (i.e., the phase boundary); the other energy scale at the QCP is the inverse of the system size. To the best of our knowledge, it is the first work that suggests that there could be a nearly perfect oscillation in the MSP even for the off-critical quenching. The above mentioned behaviors of the MSP are destroyed when impurity strength is appreciably large.

This paper is organized as follows: In Sec. II we introduce the three-spin interacting transverse field Ising model and discuss its phase diagram. We also mention the effect of an impurity term on the different phases of the model. In Sec. III, we define the quantity MSP which has been calculated for different sudden quenches. In the subsequent subsections, we illustrate our results of the MSP under an application of the impurity term for critical as well as off-critical quenches. Finally, we provide our concluding remarks in Sec. IV.

## II. MODEL

The Hamiltonian of a three-spin interacting transverse Ising model with  $N$  spins is given by [44]

$$H = -\sum_n (h\sigma_n^z + \lambda_1\sigma_n^x\sigma_{n+1}^x + \lambda_2\sigma_{n-1}^x\sigma_n^z\sigma_{n+1}^x), \quad (1)$$

where  $h$ ,  $\lambda_1$  and  $\lambda_2$  are transverse magnetic field, cooperative interaction and three-spin interaction respectively.  $\sigma^\alpha$  ( $\alpha = x, y, z$ ) are the standard Pauli matrices. This model can be exactly solved by Jordan-Wigner (JW) transformation [47] by mapping the spins into the spinless fermions. The JW transformation is defined as

$$\begin{aligned} \sigma_n^- &= \prod_{j=1}^{n-1} (-\sigma_j^z) c_n, \\ \sigma_n^z &= 2c_n^\dagger c_n - 1, \end{aligned} \quad (2)$$

where  $\sigma_n^\pm = (\sigma_n^x \pm i\sigma_n^y)/2$ , and  $c_n^\dagger$ ,  $c_n$  are the fermionic creation and annihilation operators respectively. In terms of the JW fermions, the Hamiltonian in Eq. (1) is given by

$$\begin{aligned} H &= -\sum_{n=1}^N \left[ h(2c_n^\dagger c_n - 1) - \lambda_1(c_n^\dagger c_{n+1} + c_n^\dagger c_{n+1}^\dagger + H.c.) \right. \\ &\quad \left. - \lambda_2(c_{n+1}^\dagger c_{n-1}^\dagger - c_{n-1}^\dagger c_{n+1} + H.c.) \right]. \end{aligned} \quad (3)$$

The three-spin interacting term in the Hamiltonian (1) gives rise to the next-nearest-neighbor hopping and superconducting gap terms in addition to the nearest-neighbor hopping and the superconducting gap terms. The Hamiltonian (3) reduces to a direct sum of  $2 \times 2$  decoupled Hamiltonian  $H_k$  in momentum space under the periodic boundary condition. In the momentum space representation the Hamiltonian (3) is given by

$$\begin{aligned} H &= \sum_{k>0} (c_k^\dagger \ c_{-k}) H_k \begin{pmatrix} c_k \\ c_{-k}^\dagger \end{pmatrix}, \text{ with} \\ H_k &= (h + \lambda_1 \cos k - \lambda_2 \cos 2k)\sigma^z + (\lambda_1 \sin k \\ &\quad - \lambda_2 \sin 2k)\sigma^x \end{aligned} \quad (4)$$

where  $c_k = (1/\sqrt{N}) \sum_n e^{-ikn} c_n$ . The Hamiltonian in Eq. (4) is diagonalized by a Bogoliubov transformation to obtain the energy spectrum of the system, given by

$$\varepsilon_k = \pm 2\sqrt{h^2 + \lambda_1^2 + \lambda_2^2 + 2\lambda_1(h - \lambda_2)\cos k - 2h\lambda_2\cos 2k}. \quad (5)$$

The Hamiltonian in Eq. (1) reduces to the transverse Ising model when  $\lambda_2 = 0$ ; this model has a quantum phase transition at  $\lambda_1 = h$  between a ferromagnetic and a paramagnetic phase where the energy gap vanishes for the critical modes  $k_c = \pi$ . We set  $h = 1$  throughout the paper. In order to investigate the phase diagram, as shown in Fig. (1), of the Hamiltonian (1) one has to analyze the energy spectrum in Eq. (5) as a function of  $\lambda_1$  and  $\lambda_2$ . It can be verified that the low energy excitation gap of the system vanishes on the quantum critical lines  $\lambda_2 = 1 + \lambda_1$  and  $\lambda_2 = 1 - \lambda_1$  for the critical modes  $k = 0$  and  $\pi$ , respectively. There is an another critical line  $\lambda_2 = -1$ , where the energy gap vanishes for  $k = \cos^{-1}(-\lambda_1/2)$  implying that this transition can not occur for  $\lambda_1 > 2$ . The critical line  $\lambda_2 = 1 + \lambda_1$  corresponds to the phase boundary between the three-spin dominated and ferromagnetic phases. On the other hand, the critical line  $\lambda_2 = 1 - \lambda_1$  separates the ferromagnetically ordered phase from the paramagnetic phase when  $\lambda_2 > -1$  and three-spin dominated phase for  $\lambda_2 < -1$ .

In order to explore the topological properties of the model, we represent a Jordan-Wigner fermion  $c_n$  in terms of the two Majorana fermions  $a_n$  and  $b_n$ , where

$$a_n = c_n^\dagger + c_n, b_n = -i(c_n^\dagger - c_n). \quad (6)$$

These Majorana fermions are real and satisfy the following relations  $\{a_m, a_n\} = \{b_m, b_n\} = 2\delta_{mn}$  and

$\{a_m, b_n\} = 0$ . Using the Majorana operators, the Hamiltonian in Eq. (3) with open boundary condition (OBC) can be re-written as

$$H = -i \left[ -h \sum_{n=1}^N b_n a_n + \lambda_1 \sum_{n=1}^{N-1} b_n a_{n+1} + \lambda_2 \sum_{n=2}^{N-1} b_{n-1} a_{n+1} \right]. \quad (7)$$

The three-spin interaction in Eq. (1) corresponds to a next-nearest-neighbor coupling in Majorana fermion operators that leads to an extra topological phase with two Majorana zero modes at each end of an open chain (see Fig. 1). It can be easily shown using a special condition  $h = \lambda_1 = 0$  in Hamiltonian (7) that the upper and lower three-spin dominated phases support two zero-energy Majorana edge modes at each end of the open chain:  $a_1$  and  $a_2$  exist at the left boundary, while,  $b_N$  and  $b_{N-1}$  are at the right boundary. On the other hand, in the ferromagnetic region the open chain consists one Majorana edge mode at each end i.e.,  $a_1$  at the left boundary and  $b_N$  at the right boundary. The paramagnetic region does not have any topological property, hence no edge Majorana survives in the open chain.

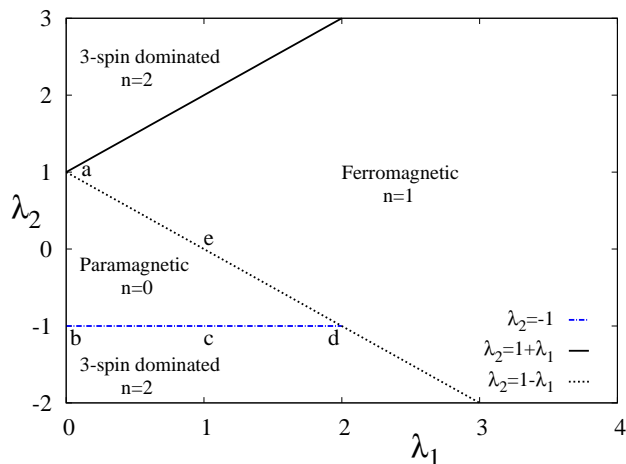


FIG. 1: (Color online) Phase diagram of the model with Hamiltonian in Eq. (1) for  $h = 1$ . The phase boundary  $\lambda_2 = 1 + \lambda_1$  separates upper topological phase (with two zero energy Majorana edge states at each end) from one Majorana ( $n = 1$ ) topological phase. The other two phase boundaries are  $\lambda_2 = 1 - \lambda_1$  ( $a - e - d$  line) and  $\lambda_2 = -1$  ( $b - d$  line). The paramagnetic region corresponds to a non-topological phase with  $n = 0$  Majorana modes. Both the topological phases with  $n = 2$  Majorana modes i.e., lower and upper, are characterized by the presence of  $a_1$  and  $a_2$  isolated modes at the left end and  $b_{N-1}$ ,  $b_N$  at the right end of the chain.

Let us now introduce some special terms in the Hamiltonian given in Eq. (7) that break the time-reversal symmetry (TRS) of the system. The total Hamiltonian containing such terms is given by

$$H_T = -i \sum_m \sum_j [K_m a_j a_{j+m} + L_m b_j b_{j+m}] + H, \quad (8)$$

where  $K_m$  and  $L_m$  are the real parameters.  $m$  denotes the range of interaction. We note that these special terms can destroy multiple number of  $a$  and  $b$  Majorana edge modes depending on the non-zero values of  $K_m$  and  $L_m$ , respectively. We here assume a simplified situation  $L_m = 0, \forall m$  and  $K_m = \lambda_d$  for a single value of  $m$ , otherwise zero. Hence, the Eq. (8) reduces to the form

$$H_T = H_{\text{imp}} + H, \text{ where} \\ H_{\text{imp}} = -i \lambda_d a_j a_q, q = j + m. \quad (9)$$

Using JW transformation  $H_{\text{imp}}$  can be expressed in terms of spin operators

$$H_{\text{imp}} = \lambda_d \prod_{n=j+1}^{j+m-1} (-\sigma_n^z) \sigma_j^y \sigma_{j+m}^x.$$

For  $m = 1$ , it reduces to  $H_{\text{imp}} = \lambda_d \sigma_j^y \sigma_{j+1}^x$  which represents the interaction between  $y$  and  $x$  components of two nearest-neighbor spins respectively. On the other hand, for larger  $m$ , it becomes non-local in terms of the spin operators. Nevertheless, in the Majorana language we can say it is quasi-local (see Eq. (9)).

In the subsequent sections, we shall refer total Hamiltonian  $H_T$  as  $H$ . It has been found that the phases with two Majorana zero modes are affected by the impurity Hamiltonian, whereas the phase with one Majorana mode remains intact. Here, the impurity term is applied in the left end of the open chain, hence the Majorana modes at the left end (i.e.,  $a$  type) vanishes but the  $b$  Majorana modes at the right end remain intact. On the other hand, if we apply the impurity in the bulk the coupling of  $a_1$  and  $a_2$  Majorana modes becomes very weak and they do not move away from zero energy.

### III. QUENCH DYNAMICS OF THE CHAIN AND RESULTS

Here, we shall study the survival probability of an edge Majorana [39] when the different terms of the Hamiltonian (7) is quenched from one phase to the other or to the QCP separating two phases as shown in Fig. 1. To study the dynamics of the zero energy edge Majorana mode after a sudden quench, we now define the Majorana survival probability (MSP)  $P_m(t)$ , defined as

$$P_m(t) = \left| \sum_{n=1}^{2N} |\langle \psi_m(\lambda_1, \lambda_2) | \Phi_n(\lambda'_1, \lambda'_2) \rangle|^2 e^{-iE_n t} \right|^2, \quad (10)$$

where  $|\psi_m(\lambda_1, \lambda_2)\rangle$  is an initial edge Majorana state for the parameters  $\lambda_1$  and  $\lambda_2$ , and  $|\Phi_n(\lambda'_1, \lambda'_2)\rangle$  are the eigenstates of the final Hamiltonian with new parameters  $\lambda'_1$ ,  $\lambda'_2$  while  $E_n$ 's are the eigenvalues of the final Hamiltonian. We study the dynamics of a zero energy edge state when the final Hamiltonian is either non-critical or critical. As mentioned already we have kept the transverse field  $h = 1$  for all the quenching processes.

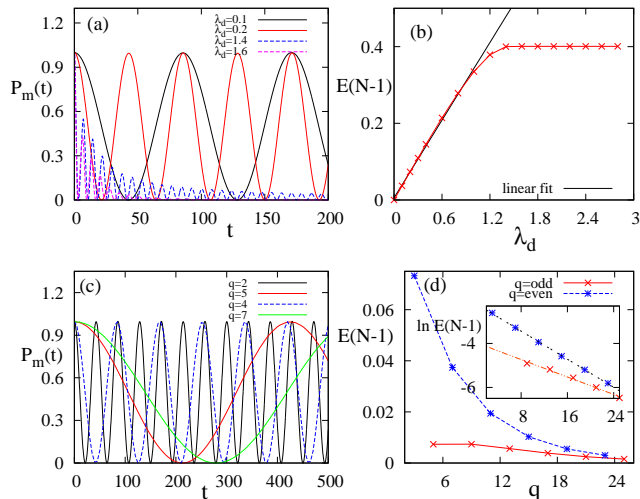


FIG. 2: (Color online) (a) The MSP of an initial zero energy edge Majorana ( $a_1$ ) shows perfect oscillation with time for smaller values of  $\lambda_d$ , whereas it decays nearly equal to zero value and does not revive significantly for higher values of  $\lambda_d$ . The rate of decay increases as the value of  $\lambda_d$  is increased. In this case, the initial Hamiltonian is considered to be in the  $n = 2$  phase with  $\lambda_1 = 0.2$  and  $\lambda_2 = 2.0$ , and the final Hamiltonian has an additional impurity term  $H_{\text{imp}} = \lambda_d a_1 a_2$  over the initial Hamiltonian. Plot (b) indicates that the energy corresponding  $a_1$  edge Majorana increases linearly with  $\lambda_d$  followed by a saturation as  $\lambda_d$  becomes large. Plot (c) shows the behavior of MSP for  $a_1$  with  $\lambda_d = 0.2$  for different interaction range of impurity term  $H_{\text{imp}} = \lambda_d a_1 a_q$  where  $q$  can take even or odd values. Plot (d) indicates that the energy corresponding the  $a_1$  Majorana decays exponentially with  $q$ . On the other hand, inset shows that the prefactor of the exponential fall is different for even and odd  $q$ . Here,  $N = 200$ .

### A. Non-critical quenching: MSP

We first discuss the effect of the impurity term (see Eq. (9)) on the MSP (10) for the case of off-critical quenching. We here investigate the MSP after a quenching inside a phase or across a phase boundary while the impurity term is added only to the final Hamiltonian.

Let us begin with a situation when the system is quenched within the upper topological phase ( $n = 2$ ) by adding an impurity term. For this quenching process the final Hamiltonian  $H_f$  is simply given by initial Hamiltonian  $H_i$  with the extra impurity term:  $H_f = H_i + H_{\text{imp}}$ . As discussed in Sec. II, the addition of such a term in Eq. (7) destroys the left end Majorana modes ( $a_1$  and  $a_2$ ) of an open chain. We are now interested to study the MSP in Eq. (10) associated with  $a_1$  Majorana mode following the above mentioned quench with  $q = 2$ . As shown in Fig. 2(a), the MSP for  $a_1$  edge Majorana shows perfect oscillations as a function of time  $t$  for smaller val-

ues of  $\lambda_d$ , whereas, the damped oscillations are observed in the case of larger values of  $\lambda_d$ . A close observation suggests that for small  $\lambda_d$ , the time period of collapse and revival in the MSP is inversely proportional to  $\lambda_d$ . Although, the Majorana zero mode  $a_1$  is not present at the final Hamiltonian, it comes back periodically at the left end of the chain with time as an outcome of the sudden quenching.

We consider the overlap function  $\alpha_n = |\langle \psi_m(\lambda_1, \lambda_2) | \Phi_n(\lambda'_1, \lambda'_2, \lambda_d) \rangle|$  of Eq. (10) to analyze this off-critical oscillation of the MSP. We find that the overlap ( $\alpha_n$ ) of an initial Majorana edge state with the  $n$ -th eigenstate of the final Hamiltonian for small  $\lambda_d$  becomes non-zero for only two values of  $n$ , i.e., the states which deviate from zero energies due to the application of the impurity term. Hence it is clear that the impurity term of smaller strength affects only two zero energy states corresponding to  $a_1$  and  $a_2$  Majorana modes and the other eigenstates remain unchanged which are indeed orthogonal to the initial edge Majorana resulting in zero overlaps.

To analyze the off-critical oscillation quantitatively, we would like to employ the degenerate perturbation theory. Let us consider the final Hamiltonian,  $H_f = H_i + H_{\text{imp}}$ , where  $H_{\text{imp}}$  can be treated as the perturbation. Then the first order correction to the zero energy of two Majorana edge states becomes  $E_{\pm} = 1/2(W_{11} + W_{22} \pm \sqrt{(W_{11} - W_{22})^2 + 4|W_{12}|^2})$ , with  $W_{11} = \langle \psi_1 | H_{\text{imp}} | \psi_1 \rangle$ ,  $W_{22} = \langle \psi_2 | H_{\text{imp}} | \psi_2 \rangle$  and  $W_{12} = \langle \psi_1 | H_{\text{imp}} | \psi_2 \rangle$ ;  $|\psi_{1/2}\rangle$  are two wavefunctions of the  $a$ -type Majorana modes at the left end of the chain that are destroyed due to the application of  $H_{\text{imp}}$ . In Majorana basis, the wavefunctions of  $a$ -type Majorana edge modes are given by  $\psi_n^T = (c_{n1}, 0, c_{n2}, 0, c_{n3}, \dots)$ , where  $n = 1, 2$  and  $c_{ni} \in \mathcal{R}$ . Since these Majorana modes are localized at the end of the chain, the value of  $|c_{ni}|^2$  falls exponentially as  $i$  is increased. Now, writing  $H_{\text{imp}}$  as given in Eq. (9) in real space matrix form, it is easy to show that  $W_{11} = W_{22} = 0$  and, only  $W_{12}$  becomes non-zero which provides  $E_{\pm} = \pm \lambda_d \sqrt{c_{2,q}^2 c_{1,j}^2 + c_{1,q}^2 c_{2,j}^2}$ . Therefore, due to the application of this small perturbation, the Majorana modes at each end mix with each other and move away from zero energy in pair [11]. One can also note that if we apply the impurity term deep inside the bulk, the edge states do not move away from zero energy, since  $|c_{ni}|^2$  decreases with increasing  $i$ . On the other hand, if the number of Majorana modes at each end is odd, one mode always remains at zero energy. In the present situation of off-critical quench, the initial edge Majorana interacts with these two non-degenerate states only and oscillates between them that reduces it to effectively a two-level problem. The time period ( $T_o$ ) of this collapse and revival is determined by the energy difference  $\Delta E$  between these two low energy levels ( $E_{\pm}$ ), given by

$$T_0 = \frac{2\pi}{\Delta E} \propto \frac{1}{\lambda_d}. \quad (11)$$

One can find that the energies associated with these

two levels increase linearly with  $\lambda_d$  up to a certain value and then there is a saturation in energy (see Fig. 2(b)) for larger values of  $\lambda_d$ . This suggests that the time period  $T_o$  of collapse and revival in the MSP is inversely proportional to  $\lambda_d$  as observed in Fig. 2(a). The above observations lead to a conclusion that when an impurity term is suddenly added in the system the initial Majorana oscillates between two Majorana sites  $a_1$  and  $a_2$  with a time period being inversely proportional to the strength of the impurity. This is an interesting observation that even for the off-critical quench the MSP shows a perfect oscillation consisting of collapse and revival as a function of time. On the other hand, for higher values of  $\lambda_d$  the MSP exhibits a damped oscillation indicating that the initial Majorana decoheres with time (see Fig. 2(a)). In these cases, we find that the overlap  $\alpha_n$  becomes non-zero even for bulk energy levels. As one increases  $\lambda_d$ , the initial edge Majorana couples with the more number of interior bulk levels and hence the temporal decay in the MSP is faster with increasing  $\lambda_d$ .

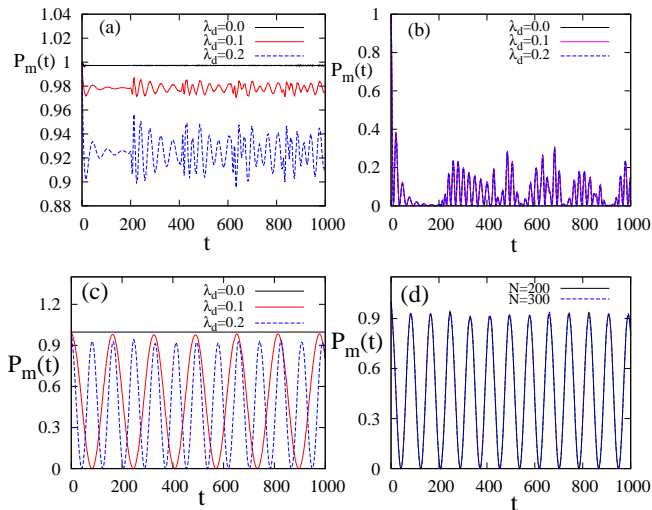


FIG. 3: (Color online) The MSP as a function of time when the system is quenched from upper  $n = 2$  phase ( $\lambda_1 = 1.8$ ,  $\lambda_2 = 3.0$ ) to  $n = 1$  phase ( $\lambda_1 = 2.2$ ,  $\lambda_2 = 3.0$ ) or vice versa. (a) The MSP of  $a_1$  Majorana mode decays initially and then becomes rapidly oscillating function of time with different mean values depending upon the values of  $\lambda_d$ . (b) On the other hand, the MSP of  $a_2$  Majorana mode decays rapidly and does not revive significantly for this quenching scheme. The plot (c) shows the MSP of  $a_1$  mode as a function of time  $t$  for smaller value of  $\lambda_d$  when the sudden quenching is carried out in the reverse path i.e., from  $n = 1$  phase to  $n = 2$  phase. We consider  $N = 200$  for the above three cases. (d) This plot indicates that the time period of the collapse and revival of the MSP here is independent of system size confirming the off-criticality of the associated dynamics. Here,  $\lambda_d = 0.2$ . For all the cases we consider  $\lambda_d a_1 a_2$  as the impurity Hamiltonian.

At the same time, we numerically calculate the MSP

using the above quenching protocol to study the effect of quasi-local impurity, i.e., when  $q > 2$  in Eq. (9). In Fig. 2(c), the MSP shows perfect collapse and revival for different values of  $q$  with  $\lambda_d = 0.2$ . We find that the logarithm of the time period of these oscillations is proportional to  $q$  (see Eq. (9));  $T_o \propto e^{\beta q}$  where the factor  $\beta$  is different for odd and even  $q$ . This form of time period can be explained by analyzing two energy levels (with non vanishing  $\alpha_n$ ) close to zero as shown in the inset of Fig. 2(d). This plot shows that the energy levels decrease exponentially as a function of  $q$  with two different values of  $\beta$  for odd and even  $q$ ; these are in good agreement with that of the obtained from  $T_o$ .

Let us now focus on the quenching from upper  $n = 2$  phase to  $n = 1$  phase and study the MSP for different values of impurity strength applied to the final Hamiltonian (see Fig. 3a,b). We numerically investigate the dynamics of both  $a_1$  and  $a_2$  Majorana modes initially existed in the upper  $n = 2$  phase. In this quenching process the MSP for  $a_1$ , shown in Fig. (3a), does not decay rather fluctuates haphazardly with a mean value close to unity. This is due to the fact that  $a_1$  Majorana mode in the  $n = 1$  phase remains unaffected in the presence of the impurity term. A pair of Majorana modes ( $a_1$  and  $b_N$ ) exists at two ends of the chain even on the critical line  $\lambda_2 = 1 + \lambda_1$  separating upper  $n = 2$  and  $n = 1$  topological phases which continues to the  $n = 1$  phase also. Therefore, in the true sense  $\lambda_2 = 1 + \lambda_1$  is not a phase boundary for the  $a_1$  edge Majorana mode. It is noteworthy that the mean value of the MSP decreases as one increases  $\lambda_d$  in the final Hamiltonian. On the other hand, the MSP for  $a_2$  mode decays rapidly to zero and remains at zero with some irregular oscillations for the above quenching process (see Fig. (3b)), since the  $n = 1$  phase does not have  $a_2$  Majorana edge mode. The different curves of the MSP for various values of  $\lambda_d$  fall on top of each other, thus confirming that the  $n = 1$  phase remains unaffected by the application of  $\lambda_d$ .

We now perform a rapid quench following the inverse path as compared to previous one, i.e., the initial Hamiltonian is in phase  $n = 1$  while the final Hamiltonian is in phase  $n = 2$  with an impurity term  $H_{\text{imp}} = \lambda_d a_1 a_2$ . As shown in Fig. 3(c), the MSP for  $a_1$  mode with  $\lambda_d = 0$  remains unity as a function of time. This is due to the fact that  $a_1$  Majorana mode exists in the phase  $n = 2$  when the impurity term is not applied there. In contrast, we find that the MSP shows collapse and revival with time having time period  $T_o \propto \lambda_d^{-1}$  when an impurity term of smaller strength is applied in the final Hamiltonian. This also can be explained with the same lines of arguments as given for Fig. 2(a). Similar to the case of off-critical quenching inside the same phase, here also, the MSP displays damped oscillations when  $\lambda_d$  becomes large. The signature of off-criticality of the dynamics is depicted in Fig. (3d) showing that collapse and revival nature of MSP is independent of  $N$ .

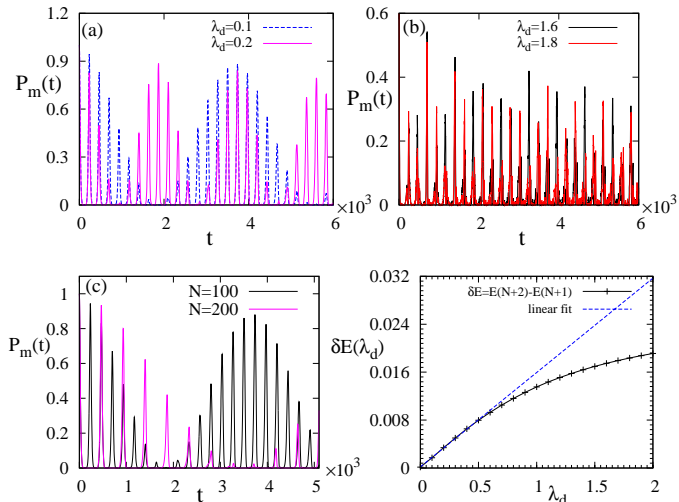


FIG. 4: (Color online) Variation of the MSP of a zero-energy Majorana mode ( $a_1$ ) as a function of time when the Hamiltonian is quenched from lower  $n = 2$  phase ( $\lambda_1 = 1.0$ ,  $\lambda_2 = -1.1$ ) to the QCP ( $\lambda_1 = 1.0$ ,  $\lambda_2 = -1.0$ ) lying on  $b-d$  line. (a) Beating pattern in the MSP as a function of time when the impurity term of small magnitude is applied along with the final Hamiltonian. It can be observed that the time-period of the envelope of the beating structure varies as  $T_{r,2} \propto 1/\lambda_d$ . (b) On the other hand, for larger values of  $\lambda_d$  one can not find any beating pattern in the MSP. Here,  $N = 100$  for the above two plots. Figure (c) depicts that the interior frequency of oscillation in the beating pattern is linearly dependent on  $N$ . Here,  $\lambda_d = 0.1$ . (d) Variation of the energy difference between two consecutive energy levels of low lying states as a function of  $\lambda_d$ . For all the above cases we consider  $\lambda_d a_1 a_2$  as the impurity term.

## B. Critical quenching: MSP

In this section, we study the MSP when the system is suddenly quenched up to a critical point with an additional impurity term  $H_{\text{imp}}$  in the final Hamiltonian. We shall restrict our focus only on the Majorana mode which is destroyed by the application of  $\lambda_d$  in phase  $n = 2$ , i.e.,  $a_1$  and  $a_2$  modes that give interesting results.

Let us first investigate the time evolution of the Majorana modes  $a_1$  and  $a_2$  under the sudden quenching from  $n = 2$  phase to  $(n = 2) - (n = 0)$  phase boundary designated by  $bcd$  line of the phase diagram (see Fig. 1). As shown in Fig. 4(a,c), MSP exhibits a beating like structure as a function of time for the critical quench with a small impurity term in the final Hamiltonian. This implies that the system has two different energy scales or frequencies in such situation. A close observation of Fig. 4(a,c) suggests that these two frequencies are related to the system size  $N$  and impurity strength  $\lambda_d$ . At the critical point, the energy levels close to zero energy are inversely proportional to the system size, i.e.,

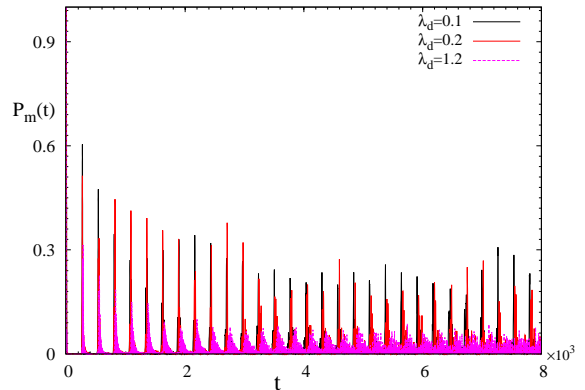


FIG. 5: (Color online)  $P_m(t)$  for  $a_1$  Majorana mode as a function of time  $t$  for the quenching from upper  $n = 2$  phase ( $\lambda_1 = 0.2$ ,  $\lambda_2 = 2$ ) to  $(n = 2) - (n = 1)$  phase boundary ( $\lambda_1 = 1$  and  $\lambda_2 = 2$ ) for different values of  $\lambda_d$  with impurity term  $H_{\text{imp}} = \lambda_d a_1 a_2$  in the final Hamiltonian. In this case the MSP does not exhibit any beating pattern and also the revival structure destroys with increasing value of  $\lambda_d$ .

$E \propto N^{-1}$ . On the other hand, similar to the case of off-critical quench, here also the application of  $\lambda_d$  gives rise to another energy scale in the system.

We shall now analyze the beating phenomena of the MSP in detail. We have found that there are two types of energy differences between two consecutive low lying energy levels of the critical Hamiltonian: one is marked by  $\delta E_L$  whose value is larger than the other one ( $\delta E_S$ ). We find that the smaller energy difference  $\delta E_S \propto \lambda_d$  for a fixed  $N$  and  $\delta E_S \propto N^{-1}$  for a fixed  $\lambda_d$ . On the other hand,  $\delta E_L$  is very weakly dependent on  $\lambda_d$  rather strongly proportional to  $N^{-1}$  with changing  $N$ . For small  $\lambda_d$ , these two energy differences remain almost constant over a few low-energy levels for which the overlap function  $\alpha_n$  becomes non-zero. As a result, the non-zero contribution in the summation of Eq. (10) arises due to the overlap of the Majorana edge mode with a few low-energy bulk states which have two types of equispaced energy levels (with the corresponding consecutive energy differences  $\delta E_L$  and  $\delta E_S$ ) alternatively. These two constant energy differences is the key factor to provide two frequencies in the non-equilibrium dynamics of the system. As mentioned already, the relatively shorter time period of the interior oscillations in the MSP is governed by the larger energy difference  $\delta E_L$ :  $T_{r,1} \sim 2\pi/\delta E_L \propto N$ , whereas, the larger time period of the envelope is  $T_{r,2} \sim 2\pi/\delta E_S \propto \lambda_d^{-1}$  or  $N$ . Therefore, we can conclude that only  $N$  controls the interior frequency and the envelope frequency of the MSP is dependent on both  $N$  and  $\lambda_d$ . For the case of  $\lambda_d \rightarrow 0$ , the value of  $\delta E_S$  is very small and we find  $\delta E_L/\delta E_S \sim O(10^2)$  leading to  $T_{r,2}/T_{r,1} \sim O(10^2)$ . We find that the time-period of the envelope associated with the beating structure for  $\lambda_d \rightarrow 0$  is very large compared to the interior oscillation.

One can intuitively understand the oscillation in

the MSP that depends on  $N$  for the critical quenching. Considering periodic boundary condition without the impurity term, the Loschmidt echo in momentum representation can be represented as  $\mathcal{L}(t) = \prod_{k>0} (1 - B_k \sin^2(E_k t))$ , where  $B_k$  is a very slowly varying positive function of the momentum  $k$  [39, 48]. Now as long as the dispersion  $E_k$  is linearly dependent on  $k$  near the critical mode, the revival time  $t_k = \frac{1}{2} p N |\partial E_k / \partial k|$  for each  $k$  becomes independent of  $k$ , with  $p$  being an integer. The MSP is indeed the Loschmidt echo with the initial ground state replaced by the initial zero energy edge Majorana state [39]; therefore, MSP follows the similar kind of behavior in the critical quenching. Hence, in addition to the  $\lambda_d$  energy scale which is also appeared in the off-critical quench, here  $N$  dependent energy scale comes into play in the dynamics resulting in to the beating structure in the MSP.

On the other hand, for larger values of  $\lambda_d$ , the overlap  $\alpha_n$  remains non-zero for more number of low energy bulk modes as compared to the case of small  $\lambda_d$ . Also,  $\delta E_S$  and  $\delta E_L$  do not remain constant (rather become irregular) for all these bulk energy states for which the overlap  $\alpha_n$  is non-zero. As a result, we do not get any prominent beating like pattern in time evolution of the MSP (see Fig. 4(b)). We have also shown that the energy difference ( $\delta E$ ) between two consecutive low lying energy levels varies linearly for small values of  $\lambda_d$ , whereas it becomes non-linear for higher  $\lambda_d$  (see Fig. 4(d)). Although, in Fig. 4(d), we have shown only one consecutive energy difference, the nature of the plot remains almost same for other few low lying energy levels.

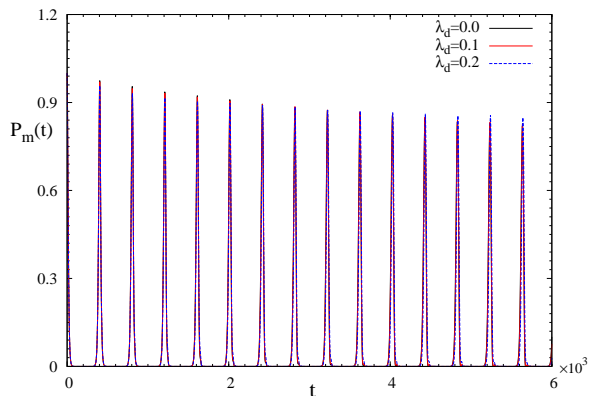


FIG. 6: (Color online) Time evolution of the MSP of a zero-energy Majorana mode ( $a_1$ ) becomes independent of the impurity strength  $\lambda_d$  when the Hamiltonian is quenched from  $n = 1$  phase ( $\lambda_1 = 1.0$ ,  $\lambda_2 = 0.2$ ) to the QCP ( $\lambda_1 = 1.0$ ,  $\lambda_2 = 0.0$ ) lying on the  $a - d$  phase boundary. Here,  $N = 200$ .

Our next aim is to investigate the behavior of MSP under the quenching from  $n = 2$  phase to  $(n = 2) - (n = 1)$  phase boundary. As shown in Fig. 5, for this case the MSP of the  $a_1$  zero-energy Majorana mode does not show a beating pattern even for the smaller values of  $\lambda_d$ . There

exists mainly one type of consecutive energy difference i.e.,  $\delta E \sim \delta E_L \sim \delta E_S$ . We observe that  $\delta E \sim N$  (for fixed  $\lambda_d$ ) though it becomes nearly independent on  $\lambda_d$  except for the level nearest to the zero energy. Hence the interference effect results in a collapse and revival type of behavior rather than a beating pattern; the time period of the revival is linearly proportional to  $N$ . We also observe that the revival structure of the MSP destroys for larger values of  $\lambda_d$ . With increasing value of  $\lambda_d$ , the  $\delta E$  changes more rapidly even for the low-energy levels. As a result, the terms of the summation in Eq. (10) interfere destructively and the revival structure of the MSP destroys with increasing  $\lambda_d$ .

We also investigate the MSP following the quenching to the  $(n = 0) - (n = 1)$  phase boundary ( $aed$  line of the phase diagram as shown in Fig. 1) starting from  $n = 1$  phase. Here, we do not observe any beating like structure in the MSP as the impurity can not give rise to another new energy scale other than the regular energy scale determined by  $N$ . As shown in Fig. (6), we find that the MSP displays a perfect collapse and revival with the revival time period  $T_r \propto N$ . It also has been observed that the MSP curves for different impurity strengths overlap with each other suggesting the fact that the energy levels of the system on the  $(n = 1) - (n = 0)$  phase boundary remain unaffected by  $\lambda_d$ . In this situation, the system contains only one energy difference  $\delta E \sim \delta E_L \sim \delta E_S$  which is inversely proportional to  $N$  and independent of  $\lambda_d$ .

We can now make a comment after a rigorous inspection of all the critical quenching cases that the beating like nature is an outcome of the existence of two types of consecutive energy difference in the low lying levels namely,  $\delta E_S$  and  $\delta E_L$ . The frequencies of the envelope and interior oscillations are dependent on the behavior that how  $\delta E_S$  and  $\delta E_L$  vary with  $N$  and  $\lambda_d$ . On the other hand, the regular collapse and revival of MSP is observed when there exists only one type of energy difference  $\delta E$  between consecutive levels;  $\delta E$  is inversely proportional to  $N$  and nearly independent of  $\lambda_d$ .

#### IV. CONCLUSIONS

In summary, we consider a next-nearest-neighbor interacting  $p$ -wave superconductor derived from a three-spin interacting Ising model in presence of a transverse field; we investigate the effect of an impurity term in the evolution of the MSP following different sudden quenches. It already has been shown that the impurity term that we have considered changes the topological nature of the topologically non-trivial phase with two zero-energy Majorana modes [45]. We have found perfect oscillation of the MSP as a function of time when an impurity term of small magnitude is applied in the system residing in a topological phase with two Majorana modes at each end. We attribute this phenomena of perfect oscillation of Majorana, even though the final system remains at a

off-critical point, to the coupling of the initial Majorana state with only two energy levels close to zero energy of the final Hamiltonian. As a result, this eventually reduces to the two-level problem.

Additionally, we find that there exists two types of bulk energy difference of two consecutive equispaced low-energy states on the  $(n = 0) - (n - 2)$  phase boundary. This leads to a nice beating like structure in the MSP when the system is quenched from two edge Majorana phase to the  $(n = 0) - (n = 2)$  phase boundary. The underlying two frequencies that generate the beating structure are connected with the impurity strength and the system size. The beating pattern becomes ir-

regular when the strength of the impurity is increased appreciably since the Majorana state then starts mixing with higher energy bulk states which are not equispaced.

### Acknowledgments

We sincerely thank Amit Dutta and Bikas K. Chakrabarti for fruitful discussion regarding the work. AR and TN thank IIT Kanpur and SINP Kolkata respectively for providing hospitality during the part of this work.

- 
- [1] E. Majorana, *Nuovo Cimento* **5**, 171 (1937).  
 [2] A. Kitaev and C. Laumann, arXiv:0904.2771v1 (2009).  
 [3] J. C. Budich, S. Walter and B. Tranzettel, *Phys. Rev. B* **85**, 121405 (R) 2012.  
 [4] M. J. Schmidt, D. Rainis and D. Loss, *Phys. Rev. B* **86**, 085414 (2012).  
 [5] S. Tewari, S. D. Sarma, C. Nayak, C. Zhang, and P. Zoller, *Phys. Rev. Lett.* **98**, 010506 (2007).  
 [6] A. Kitaev, *Physics-Uspekhi* **44**, 131 (2001), arXiv:cond-mat/0010440v2 (2000).  
 [7] I. C. Fulga, F. Hassler, A. R. Akhmerov, and C. W. J. Beenakker, *Phys. Rev. B* **83**, 155429 (2011).  
 [8] J. D. Sau and S. Das Sarma, *Nature communications* **3**, 964 (2012).  
 [9] R. M. Lutchyn and M. P. A. Fisher, *Phys. Rev. B* **84**, 214528 (2011).  
 [10] W. DeGottardi, D. Sen, and S. Vishveshwara, *New J. Phys.* **13**, 065028 (2011).  
 [11] W. DeGottardi, D. Sen, and S. Vishveshwara, *Phys. Rev. Lett.* **110**, 146404 (2013).  
 [12] M. Thakurathi, A.A. Patel, D. Sen, and A. Dutta, *Phys. Rev. B* **88**, 155133 (2013).  
 [13] W. DeGottardi, M. Thakurathi, S. Vishveshwara, and D. Sen, *Phys. Rev. B* **88** 165111 (2013).  
 [14] J. Alicea, *Rep. Prog. Phys.* **75**, 076501 (2012).  
 [15] L. Fu and C.L. Kane, *Phys. Rev. Lett.* **100**, 096407 (2008).  
 [16] M. Z. Hasan and C.L. Kane, *Rev. Mod. Phys.* **82**, 3045 (2010).  
 [17] X.-L. Qi and S.-C. Zhang, *Rev. Mod. Phys.* **83**, 1057 (2011).  
 [18] V. Mourik et al., *Science* **336**, 1003 (2012).  
 [19] M.T. Deng, C.L. Yu, G.Y. Huang, M. Larsson, P. Caroff, and H.Q. Xu, *Nano Lett.* **12**, 6414 (2012).  
 [20] A. Das, Y. Ronen, Y. Most, Y. Oreg, M. Heiblum, and H. Shtrikman, *Nat. Phys.* **8**, 887 (2012).  
 [21] W. Chang, V. Manucharyan, T. Jespersen, J. Nygard, and C. Marcus, *Phys. Rev. Lett.* **110**, 217005 (2013).  
 [22] E. J. H. Lee, X. Jiang, M. Houzet, R. Aguado, C. M. Lieber, and S. De Franceschi, *Nature Nanotechnol* **9**, 79-84 (2014).  
 [23] D. Rainis, L. Trifunovic, J. Klinovaja, and D. Loss, *Phys. Rev. B*, **87**, 024515 (2013).  
 [24] A. D. K. Finck, D. J. Van Harlingen, P. K. Mohseni, K. Jung, and X. Li, *Phys. Rev. Lett.* **110**, 126406 (2013).  
 [25] A. Dutta, G. Aeppli, B. K. Chakrabarti, U. Divakaran, T. Rosenbaum and D. Sen, *Quantum Phase Transitions in Transverse Field Spin Models: From Statistical Physics to Quantum Information* (Cambridge University Press, Cambridge, 2015).  
 [26] A. Bermudez, D. Patan, L. Amico, M. A. Martin-Delgado, *Phys. Rev. Lett.* **102**, 135702 (2009).  
 [27] A. Bermudez, L. Amico, and M.A. Martin-Delgado, *New J. Phys.* **12**, 055014 (2010).  
 [28] P. Wang, W. Yi, and G. Xianlong, arXiv: 1404.6848v1 (2014).  
 [29] F. Setiawan, K. Sengupta, I.B. Spielman, and Jay D. Sau, *Phys. Rev. Lett.* **115**, 190401 (2015).  
 [30] N. Wu, A. Nanduri, and H. Rabitz *Phys. Rev. B*, **91**, 041115 (2015).  
 [31] P. D. Sacramento, *Phys. Rev. E*, **90**, 032138 (2014).  
 [32] P. D. Sacramento, *Phys. Rev. B*, **91**, 214518 (2015).  
 [33] L. Dai and M-C Chung, *Phys. Rev. A*, **91**, 062319 (2015).  
 [34] A. A. Zvyagin, *Phys. Rev. B*, **92**, 184507 (2015).  
 [35] S. Hegde, V. Shivamoggi, S. Vishveshwara, and D. Sen, *New J. Phys.* **17** (2015) 053036.  
 [36] P. Wang, W. Yi and G. Xianlong, *New J. Phys.* **17**, 013029 (2015).  
 [37] U. Bhattacharya and A. Dutta, arXiv: 1610.02674 (2016).  
 [38] M. Lee, S. Han and M-S. Choi, *New J. Phys.* **18**, 063004 (2016).  
 [39] A. Rajak and A. Dutta, *Phys. Rev. E* **89**, 042125 (2014).  
 [40] A.A. Patel, S. Sharma, and A. Dutta, *Eur. Phys. J. B* **86**, 367 (2013).  
 [41] P. D. Sacramento, *Phys. Rev. E*, **93**, 062117 (2016).  
 [42] E. Perfetto, *Phys. Rev. Lett.* **110**, 087001 (2013).  
 [43] A. Rajak, T. Nag and A. Dutta, *Phys. Rev. E* **90**, 042107 (2014).  
 [44] A. Kopp and S. Chakravarty, *Nat. Phys.*, **1**, 53 (2005).  
 [45] Y. Niu, S. K. Chung, C-H Hsu, I. Mandal, S. Raghu and S. Chakravarty, *Phys. Rev. B*, **85**, 035110 (2012).  
 [46] A. Bayat, S. Bose, H. Johannesson, and P. Sodano, *Phys. Rev. B* **92**, 155141 (2015).  
 [47] E. Lieb, T. Schultz, and D. Mattis, *Ann. Phys.*, **16**, 37004 (1961).  
 [48] J. Happola and G. B. Halasz and A. Hamma, *Phys. Rev. A* **85**, 032114 (2012).